

# kNNDM: k-fold Nearest Neighbour Distance Matching Cross-Validation for map accuracy estimation

Jan Linnenbrink<sup>1,\*</sup>, Carles Milà<sup>2,3\*</sup>, Marvin Ludwig<sup>1</sup>, and Hanna Meyer<sup>1</sup>

<sup>1</sup>Institute of Landscape Ecology, University of Münster, Münster, Germany

<sup>2</sup>Barcelona Institute for Global Health (ISGlobal), Barcelona, Spain

<sup>3</sup>Universitat Pompeu Fabra (UPF), Barcelona, Spain

\*These authors contributed equally to this work.

**Correspondence:** Jan Linnenbrink (jan.linnenbrink@uni-muenster.de)

**Abstract.** Random and spatial Cross-Validation (CV) methods are commonly used to evaluate machine learning-based spatial prediction models, and the obtained performance values are often interpreted as map accuracy estimates. However, the appropriateness of such approaches is currently the subject of controversy. For the common case where no probability sample for validation purposes is available, in Milà et al. (2022) we proposed the Nearest Neighbour Distance Matching (NNDM) Leave-One-Out (LOO) CV method. This method produces a distribution of geographical Nearest Neighbour Distances (NND) between test and train locations during CV that matches the distribution of NND between prediction and training locations. Hence, it creates predictive conditions during CV that are comparable to what is required when predicting a defined area. Although NNDM LOO CV produced largely reliable map accuracy estimates in our analysis, as a LOO-based method, it cannot be applied to large datasets found in many studies.

Here, we propose a novel k-fold CV strategy for map accuracy estimation inspired by the concepts of NNDM LOO CV: the k-fold NNDM (kNNDM) CV. The kNNDM algorithm tries to find a k-fold configuration such that the Empirical Cumulative Distribution Function (ECDF) of NND between test and train locations during CV is matched to the ECDF of NND between prediction and training locations.

We tested kNNDM CV in a simulation study with different sampling distributions and compared it to other CV methods including NNDM LOO CV. We found that kNNDM CV performed similarly to NNDM LOO CV and produced reasonably reliable map accuracy estimates across sampling patterns with strong reductions in computation time for large sample sizes. Furthermore, we found a positive association between the quality of the match of the two ECDFs in kNNDM and the reliability of the map accuracy estimates.

kNNDM provided the advantages of our original NNDM LOO CV strategy while bypassing its sample size limitations.

## 1 Introduction

Spatial predictive modeling using machine learning methods is commonly used in ecology and environmental sciences to predict variables sampled at a limited set of locations to new, unobserved locations (see e.g. van den Hoogen et al., 2019; Sabatini et al., 2022; Moreno-Martínez et al., 2018; Hengl et al., 2017, for global studies). A key step in the spatial prediction

workflow is the map accuracy assessment, i.e. the process whereby the quality of a prediction of a spatially-indexed variable  
25 in a finite and defined geographical area (e.g. a set of pixels forming a continuous surface) is estimated (Stehman et al.,  
2021; Wadoux et al., 2021). Although map accuracy assessment should ideally be done via design-based inference based on  
probability sampling (Wadoux et al., 2021), this is frequently not possible due to limited access to certain areas or expensive  
sampling methods (Martin et al., 2012). Instead, Cross-Validation (CV) methods are commonly used to estimate map accuracy.  
Previous studies, however, showed significant differences in map accuracy estimates depending on the type of CV being used,  
30 which initiated discussions on the appropriateness of these strategies (Wadoux et al., 2021; Meyer and Pebesma, 2022; Milà  
et al., 2022; Roberts et al., 2017; Ploton et al., 2020). Since CV is also typically used during model development (i.e during  
hyperparameter tuning (Schratz et al., 2019) and feature selection (Meyer et al., 2019)), reliable estimates of map accuracy are  
crucial to develop suitable prediction models.

Traditional CV methods that ignore the spatial structure of the data such as Leave-One-Out (LOO) or random k-fold CV  
35 (Hastie et al., 2009) have been found to provide reliable estimates of map accuracy when samples are randomly distributed  
within the entire prediction area, but not when they are clustered (Milà et al., 2022; Wadoux et al., 2021) or only covering  
parts of the prediction area (Meyer and Pebesma, 2021). As an alternative, spatial CV methods such as block CV (Wenger  
and Olden, 2012; Valavi et al., 2019; Roberts et al., 2017) or buffered-LOO CV (Telford and Birks, 2009; Le Rest et al.,  
2014; Brenning, 2022) are often used. Spatial CV methods are designed for geographical model transferability assessment,  
40 i.e. to test the ability of the model to make predictions for new geographic entities far away from the sampling areas, by  
designing a CV where independence between train and test data is sought (Roberts et al., 2017). Such strategies, however,  
have been found to underestimate map accuracy when reference data are regularly or randomly distributed within the entire  
prediction area. In some cases, this has been even reported for clustered samples (Wadoux et al., 2021; Milà et al., 2022).  
Recent proposals of methods for map accuracy estimation include sampling-intensity weighted CV, as well as model-based  
45 geostatistical approaches (de Bruin et al., 2022). However, the results of de Bruin et al. (2022) showed that these methods are  
not universal solutions and, depending on the sampling design, showed considerable over- or underestimation of the true map  
accuracy.

In our past work, we argued that the design of a CV method to provide a reliable estimate for map accuracy should be  
prediction-oriented, i.e. predictive conditions created during CV should resemble the conditions found when the trained model  
50 is applied to the prediction area (Milà et al., 2022; Meyer and Pebesma, 2022; Ludwig et al., 2023). Following this idea, in  
Milà et al. (2022) we considered predictive conditions in terms of geographical distances, and proposed the Nearest Neighbour  
Distance Matching (NNDM) LOO CV method, a prediction-oriented CV method based on spatial point patterns concepts (Milà  
et al., 2022). Briefly, NNDM aims to match the Empirical Cumulative Distribution Function (ECDF) of Nearest Neighbour  
Distances (NND) between test and train locations in the CV, to the ECDF of NND between prediction and training locations  
55 found during prediction.

In Milà et al. (2022) we showed that when standard LOO CV is used for randomly distributed reference data within the  
prediction area, the distribution of NND between test and training locations during CV is similar to the distribution of NND  
between prediction and training locations (see Meyer and Pebesma, 2022, for similar results for random k-fold CV). In the

case of clustered sampling designs, NND during LOO CV were generally much shorter than prediction NND which led to significant error underestimation (see also Ludwig et al., 2023). For regular samples, NND during LOO CV were found to be slightly longer than during prediction leading to slight error overestimation (Milà et al., 2022). With the newly developed NNDM LOO CV, we could produce comparable NND distributions in most sampling designs and provide more reliable estimates of map accuracy that can be used during model development or to indicate the accuracy of the predictions.

Even though our proposed method showed promising results across different sampling designs, prediction areas, and landscape autocorrelation ranges (Milà et al., 2022), the fact that it is a LOO-based CV method hinders its broader application given its high computational cost in medium and large datasets. To overcome this limitation, our aim is to extend the idea of NNDM LOO CV to a  $k$ -fold NNDM CV, hereafter kNNDM, that can be applied to larger datasets commonly found in ecology and the environmental sciences.

This article is organised as follows: after presenting our algorithm in section 2, in section 3 we reproduce the simulation study included in Milà et al. (2022) to assess the performance and runtime of kNNDM compared to other CV methods including NNDM LOO. In this simulation, we also explore the influence of the number of folds  $k$  and the relationship between the quality of the match and the quality of the estimation of the map accuracy. As supplementary material, we provide a second simulation study which we also briefly describe in section 3. Finally, section 4 discusses the strengths and limitations of our method and suggests future lines of work.

## 75 2 Algorithm description

The algorithmic objective of kNNDM is the same as in the original NNDM LOO approach: to match the ECDF of the NND between test and training locations during CV, to the ECDF of NND between prediction and training locations found during prediction. While in the original NNDM LOO approach we focused on matching NND ECDF up to the range of the residual spatial autocorrelation of the variable being modelled (Milà et al., 2022), here we match all the ECDF to avoid the complexity and possible pitfalls of semivariogram estimation (e.g. trend, anisotropy, sampling size and spacing, preferential sampling; see Webster and Oliver (2007) for an overview). We define distances as Euclidean for projected coordinates and spherical for geographical coordinates.

In kNNDM, the definitions of the different NND ECDF remain the same as in the original NNDM LOO algorithm, where  $j$  is the index for training points and  $i$  is the index for prediction points (see detailed definitions with equations in Milà et al. (2022)):

- $\hat{G}_j(r)$  is the NND ECDF between test and train locations during LOO CV and expresses the proportion of training points that have another training point at a distance equal or lower than  $r$ .
- $\hat{G}_{ij}(r)$  is the NND ECDF between prediction and training locations and expresses the proportion of prediction points that have a sampling point at a distance equal or lower than  $r$ .
- $\hat{G}_j^*(r, \mathbf{L})$  is the NND ECDF between test and train locations during a CV defined in  $\mathbf{L}$  and expresses the proportion of test points that have a training point at a distance equal or lower than  $r$  during a given CV strategy. Note that  $\mathbf{L} =$

$\{\mathbf{l}_1, \mathbf{l}_2, \dots, \mathbf{l}_{n_j}\}$  is a list of sets  $\mathbf{l}_j$  containing the indices of the samples to fit the model to when holding out observation  $j$  during CV. Note that since in kNNDM we leave out data points in folds rather than one by one,  $\mathbf{l}_j$  will be exactly the same for all samples belonging to the same fold.

95 Another important component of our approach is how to measure the quality of the match between  $\hat{G}_j^*(r, \mathbf{L})$  and  $\hat{G}_{ij}(r)$  given a fold configuration. We do that by using the Wasserstein statistic (Dowd, 2020; Vaserstein, 1969), which compares the distribution of two samples by calculating the integral of the absolute value differences between the two ECDFs. In our case, we define  $W$  as the integral over the geographical distances  $r$  of the absolute value differences between  $\hat{G}_j^*(r, \mathbf{L})$  and  $\hat{G}_{ij}(r)$ :

$$W = \int |\hat{G}_j^*(r, \mathbf{L}) - \hat{G}_{ij}(r)| dr$$

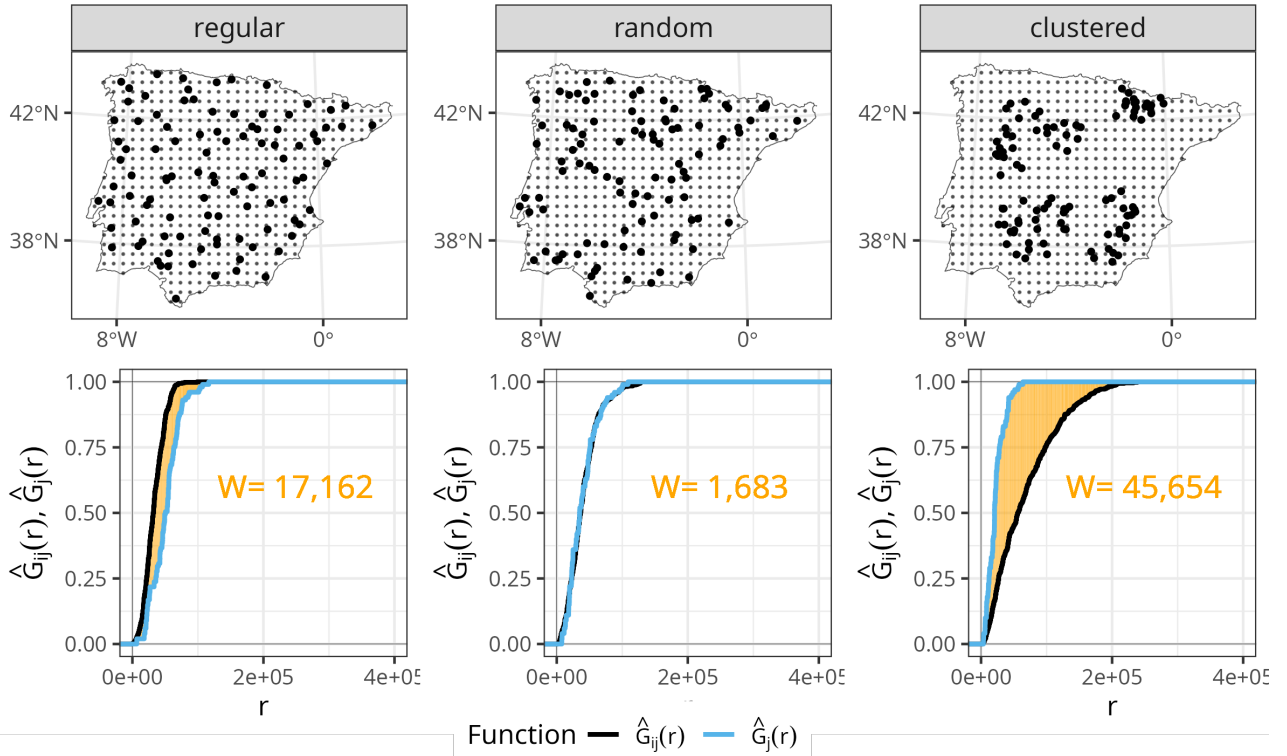


**Figure 1.** Top row: prediction points (regular grid) and simulated training points with different spatial distributions (bold). Bottom row: NND ECDF between training locations found during LOO CV ( $\hat{G}_j(r)$ , blue) and NND ECDF between prediction and training locations ( $\hat{G}_{ij}(r)$ , black) corresponding to each of the sampling distributions in the top row. The shaded yellow area corresponds to the  $W$  statistic, whose value is printed in the plots.

100 Small values of  $W$  indicate that the two ECDFs are similar, while  $W$  will be larger if they differ. To illustrate this point, we show the calculation of the  $W$  statistic between  $\hat{G}_j(r)$  (ECDF of NND during LOO CV) and  $\hat{G}_{ij}(r)$  (ECDF of NND during prediction) for different sampling patterns (Figure 1). As shown in Milà et al. (2022), when samples are randomly distributed

within the prediction area,  $\hat{G}_j(r)$  resembles  $\hat{G}_{ij}(r)$  (since  $\hat{G}_j(r) \approx \hat{F}_j(r)$  under complete spatial randomness, see Baddeley et al. (2015)) and therefore the value of  $W$  is small. However, in presence of clustered samples, LOO CV NND are shorter than prediction NND, and thus  $\hat{G}_j(r) > \hat{G}_{ij}(r)$ , resulting in a large  $W$  value. The opposite occurs when training samples follow a regular sampling pattern, also leading to a larger  $W$  statistic compared to random sampling.

The objective of the kNNDM algorithm (Figure 2) is to find a  $k$ -fold configuration such that  $W$  measuring the match between  $\hat{G}_j^*(r, \mathbf{L})$  and  $\hat{G}_{ij}(r)$  is minimised. The first step is to test whether the training points are clustered with respect to the prediction points; to do that we compute  $\hat{G}_j(r)$  and  $\hat{G}_{ij}(r)$ , and then test the null hypothesis  $G_j(r) \leq G_{ij}(r)$  vs. the alternative  $G_j(r) > G_{ij}(r)$  with a one-sided Kolmogorov–Smirnov (KS) two-sample test (Conover, 1999). If the null hypothesis is not rejected, the algorithm returns a random  $k$ -fold CV since it is the appropriate option for random and regular samples (Meyer and Pebesma, 2022; Wadoux et al., 2021; de Bruin et al., 2022). If, however, the null hypothesis is rejected ( $p$ -value  $< 0.05$ ), we proceed to cluster the training points based on their coordinates into a range of  $q_i \in Q$  clusters, where  $Q$  is defined as an integer sequence of length 100 ranging between  $k$  and  $N$  (the total number of training points) equally-spaced in the logarithmic scale and back-transformed, to try configurations with a small number of clusters more intensively. Currently, hierarchical and  $k$ -means clustering methods are implemented.

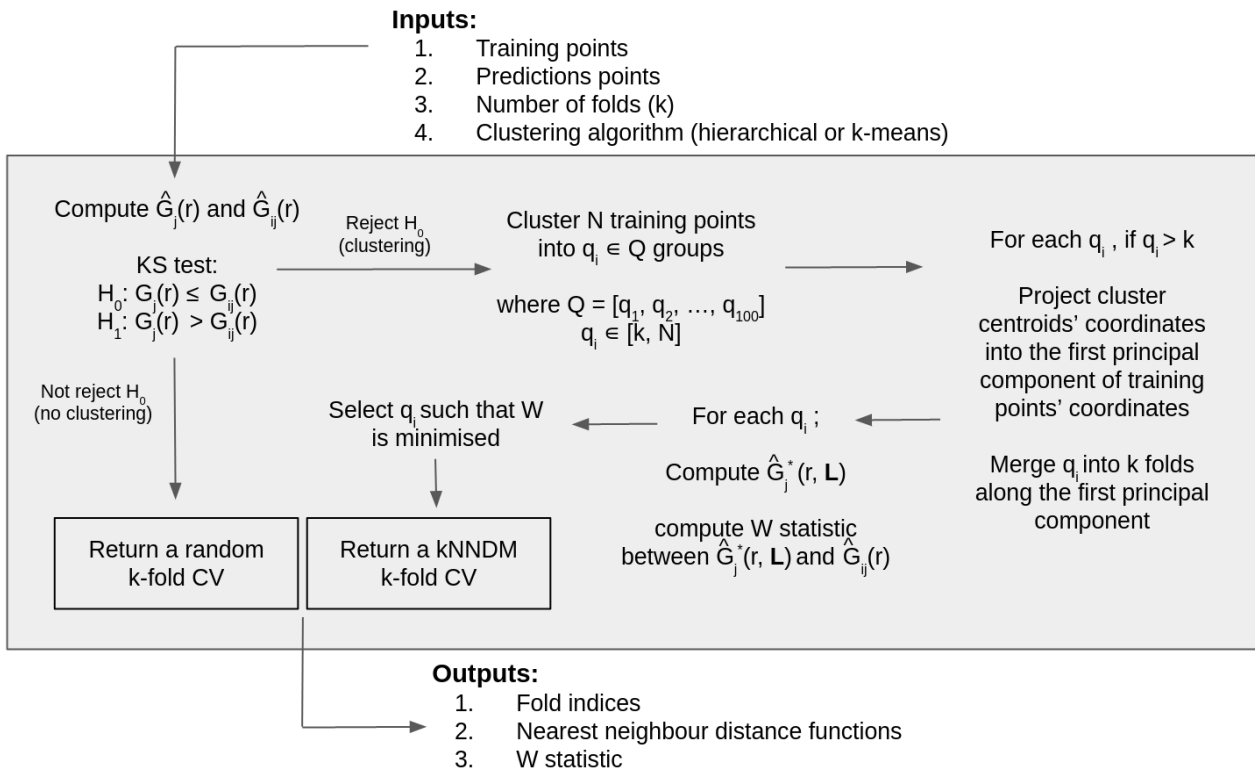


**Figure 2.** Workflow of the kNNDM algorithm.

Next, for every configuration where  $q > k$ , we merge the resulting  $q$  clusters into the final  $k$  folds along the first principal component of the training points' coordinates to prevent contiguous clusters in space to be in the same fold. Briefly, we compute the first principal component of the training points' coordinates to capture the direction with the most spatial variability, project the  $q$  cluster centroids into that first component and order them according to it, and finally merge  $q$  into  $k$  folds by giving different fold levels to contiguous clusters in that dimension. Large clusters with a proportion greater than  $1/k$  of the training data are not merged to keep fold balance. Once this procedure is completed, we compute  $\hat{G}_j^*(r, \mathbf{L})$  and  $W$  for each fold configuration candidate and select the one with the smallest  $W$ , i.e. the one that provides the best match between  $\hat{G}_j^*(r, \mathbf{L})$  and  $\hat{G}_{ij}(r)$ .

As an illustration of how kNNDM works in cases where samples are clustered within the prediction area, Figure 3 shows a 2-fold kNNDM CV configuration for different number of clusters  $q$ , their respective NND ECDF functions, and the  $W$  statistic between  $\hat{G}_j^*(r, \mathbf{L})$  and  $\hat{G}_{ij}(r)$  assessing the match. A low number of clusters leads to a strong partition of the geographical space and long NND between test and train points during CV, which are actually longer than NND encountered when predicting from all reference data. As the number of clusters increases,  $\hat{G}_j^*(r, \mathbf{L})$  gets closer to  $\hat{G}_j(r)$ , i.e. the NND ECDF encountered during LOO CV. In this example, the kNNDM algorithm would select the configuration with  $q = 21$  since it minimises the  $W$  statistic, i.e. provides the best match.

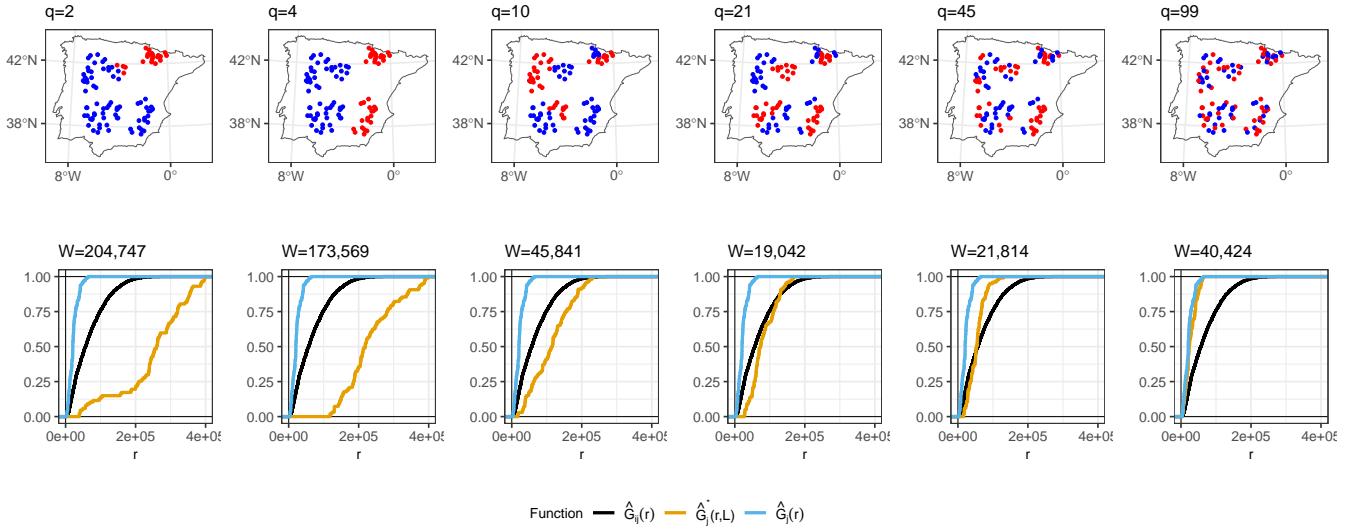


**Figure 3.** Top row: kNNDM with  $k=2$  (red and blue points) for several number of clusters  $q$ . Prediction points consist of a regular grid (not shown) spanning the whole polygon. Bottom row: NND ECDF between training locations during LOO CV ( $\hat{G}_j(r)$ , blue), between test and train locations during kNNDM CV ( $\hat{G}_j^*(r, \mathbf{L})$ , yellow), and between prediction and training locations ( $\hat{G}_{ij}(r)$ , black) corresponding to each CV configuration in the top row.

As practical considerations, in our implementation we have provided the possibility, as an alternative to the prediction points input, of supplying a polygon defining the prediction area, from which prediction points are sampled internally. Moreover, we

have included a balancing parameter for the maximum single fold size allowed that discards non-compliant fold candidates.  
135 Regarding computational performance, our algorithm benefits from using projected coordinates since fast nearest neighbour-  
hood searches in the Euclidean space can be done using the FNN package (Beygelzimer et al., 2022). Finally, when using  
kNNNDM we recommend computing accuracy statistics such as coefficient of determination ( $R^2$ ), the Root Mean Square Error  
(RMSE), or the Mean Absolute Error (MAE) in the stacked out-of-sample predictions rather than performing an average of the  
140 statistics computed in each of the folds, since the resulting folds can be unbalanced and  $\hat{G}_j^{rs*}(r, \mathbf{L})$  is constructed using all CV  
folds simultaneously (Meyer et al., 2023).

### 3 Simulation studies

#### 3.1 Algorithm performance for map accuracy estimation

To investigate the performance of kNNNDM CV and how it compares to the original NNDM LOO CV, we used the same  
simulation as in our previous work (see Milà et al. (2022) for a complete description). Briefly, we generated a virtual response  
145 surface, i.e. a spatially-indexed continuous variable between 0 and 1, using a selection of WorldClim bioclimatic variables for  
the Iberian peninsula (Figure 4A) and the `virtualSpecies` R package (Leroy et al., 2015). Next, we simulated training  
locations with five different distributions and a sample size of 100 (Figure 4B). We performed 100 iterations of the sampling  
simulation and, in each of them, we extracted the predictor (bioclimatic variables) and response data at the sampling points'  
locations and fitted Random Forest (RF) regression models, resulting in a total of 500 fitted models. RF hyperparameters were  
150 not tuned and default values were used in all simulations to shorten computation time.

Each fitted RF model was used to predict the response in the entire prediction area, from which the true map accuracy was  
calculated (RMSE, MAE and  $R^2$ ). Additionally, we used the following CV methods: 1) random 10-fold CV, 2) spatial 10-fold  
CV via k-means clustering (Brenning, 2012), 3) the original NNDM LOO CV and 4) 10-fold kNNNDM CV. In contrast to the  
original simulation in Milà et al. (2022), here we matched all distances in the prediction area during NNDM rather than up to  
155 a certain range estimated from the data. In order to interpret results, we subtracted the true map accuracy metrics from each of  
the CV estimates to assess their performance (Figure 5).

kNNNDM CV yielded reliable error estimates across all sampling patterns we considered, which were similar and in some  
cases even more accurate than those estimated via NNDM LOO CV (Figure 5). Variability of the differences was larger in  
kNNNDM than in NNDM LOO CV for strongly clustered samples. Random 10-fold CV produced reliable estimates under  
160 random sampling patterns but failed for clustered data. The spatial 10-fold CV overestimated the mapping error except for the  
RMSE in the strong clustering scenario and had the largest variability.

#### 3.2 Relationship between the quality of the match and the quality of the map accuracy estimate

In order to investigate the relationship between the quality of the match in kNNNDM and the quality of the map accuracy metrics,  
we performed a second simulation using the same response and predictors and 100 iterations of our first simulation (section

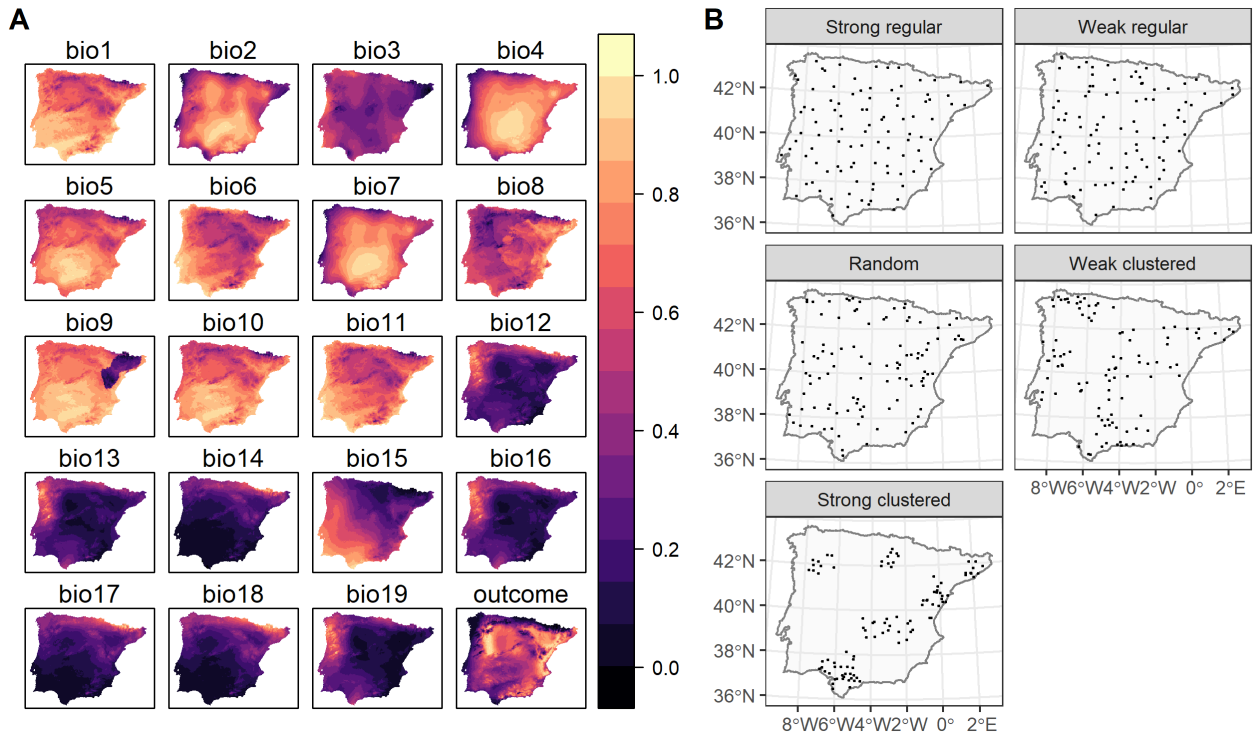


**Figure 4.** Data used in the simulation: A) bioclimatic covariates and response (all linearly stretched to [0,1] for visualization purposes); and B) example of one iteration of the sample simulation. Figure reproduced as in Milà et al. (2022).

165 3.1). However, in this second simulation, we 1) added two more extreme clustered sample configurations to extend the range  
of possible  $W$  values, 2) only used kNNDM CV, 3) did not check for clustering as a first step in kNNDM, i.e. we applied  
the clustering approach to all samples regardless of their distribution, and 4) we kept all candidate fold configurations  $q_i \in Q$   
considered within kNNDM and their respective values of the  $W$  statistic, rather than just the one yielding the lowest  $W$ . We  
used all of these candidate CV splits to calculate CV map accuracy statistics, and computed the absolute value difference with  
170 respect to the true value of the map accuracy statistic. We then plotted these absolute value differences against the corresponding  
 $W$  statistic and fitted a linear regression to summarise the trend (Figure 6).

The relationship between the absolute value differences between CV and true map accuracy statistics (Figure 6) and  $W$   
showed that, for all three statistics considered, a poor match between  $\hat{G}_j^*(r, \mathbf{L})$  and  $\hat{G}_{ij}(r)$  indicated by a greater  $W$  statistic  
led to a poor estimation of the true map accuracy, while the true map accuracy could be better estimated for well-matching  
175 functions. This positive association was linear for all three statistics with at least 60% explained variance.



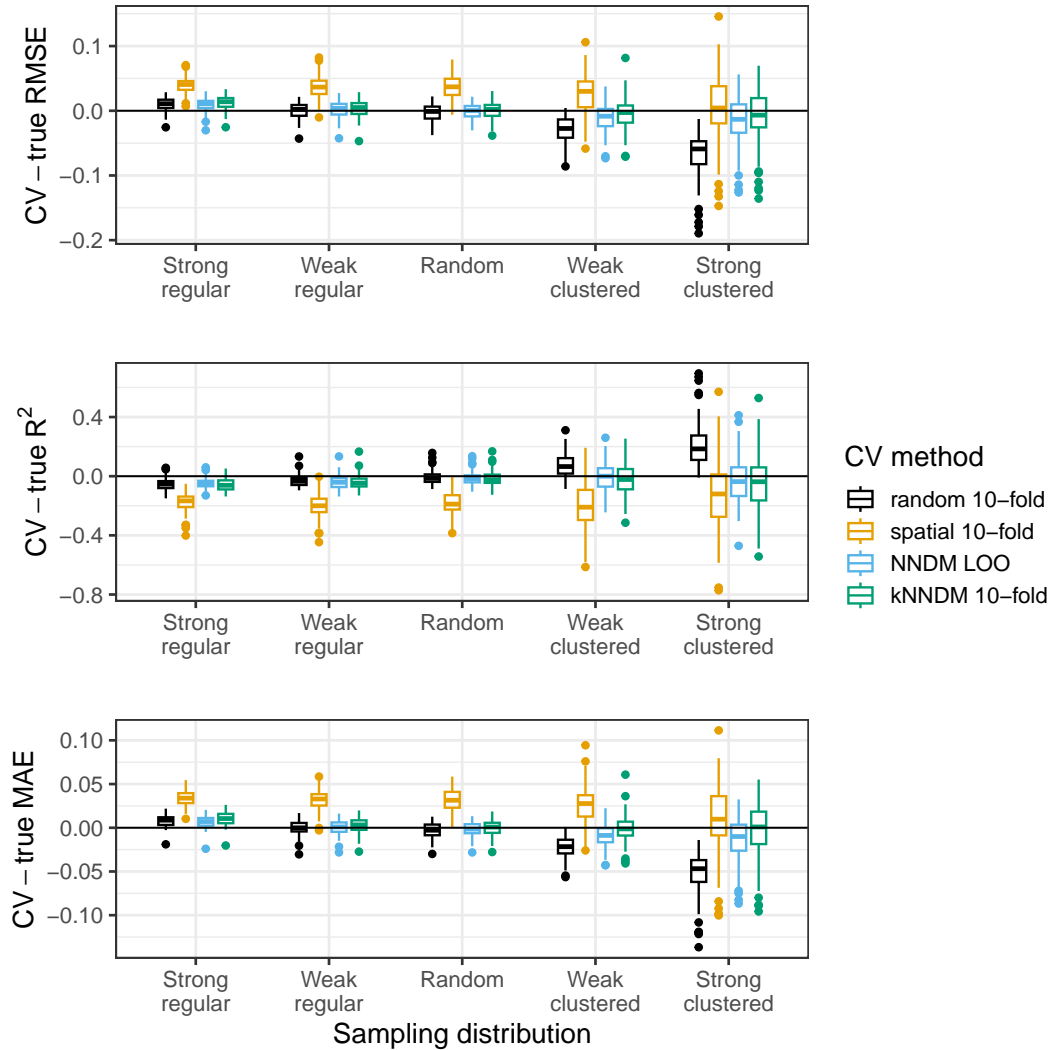


**Figure 5.** Differences between cross-validated and true RMSE,  $R^2$ , and MAE by sampling distribution and CV method for the simulated virtual response variable.

### 3.3 Influence of the number of folds

The choice of  $k$  can influence the performance of kNNDM to a certain extent since it dictates the maximum clustering that can be achieved. To investigate the influence of  $k$ , we repeated the workflow described in section 3.1 but only employed kNNDM CV using an even integer sequence  $k \in [2, 4, 6, \dots, 20]$ . In each of the 100 iterations, we calculated the true and estimated error metrics, as well as the quality of the match between the ECDF of NND between CV folds ( $\hat{G}_j^*(r, \mathbf{L})$ ) and the ECDF of NND between prediction points and sample points ( $\hat{G}_{ij}(r)$ ) as measured by the Wasserstein statistic ( $W$ ). With the resulting statistics,

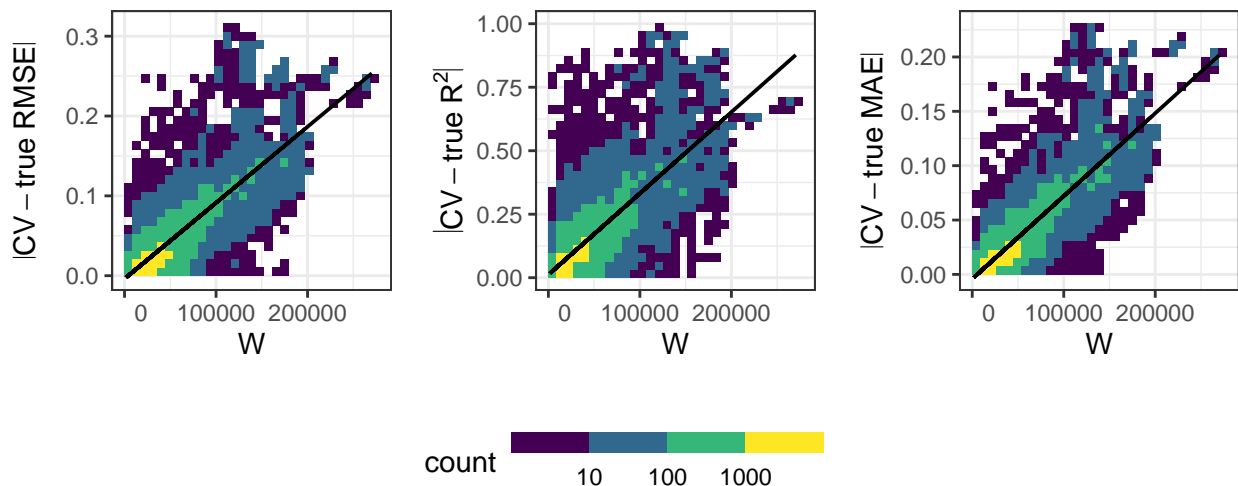


**Figure 6.** Relationship in 10-fold kNNDM between the absolute value difference between the CV and true map accuracy statistics (y-axis) and  $W$  statistic (x-axis) for the RMSE (left),  $R^2$  (centre), and MAE (right) statistics. Colour represents the data point density. The black line shows the linear regression fit. The  $R^2$  values of the regression models are 0.66, 0.6 and 0.73 for the RMSE,  $R^2$ , and MAE, respectively.

we plotted the distribution of the differences between the estimated and true RMSE, MAE, and  $R^2$  as well as the  $W$  statistic for each number of  $k$  (Figure 7).

Our results indicated that a larger number of folds resulted in better matches for regular and random samples but worse  
 185 for strongly clustered designs. While for regular and random samples this translated into increasingly accurate map accuracy estimates for larger number of folds, for clustered data, the number of folds with the smallest  $W$ , i.e.  $k = 2$  was overly pessimistic and  $k=4$  or 6 had actually a better performance.

### 3.4 Run-time analysis

Since our goal was to propose a computationally feasible alternative to NNDM LOO CV for large datasets, we performed  
 190 a run-time analysis to quantify the speed gains of kNNDM CV compared to NNDM LOO CV. We separately quantified the time spent on 1) finding the optimal CV split (i.e., running the NNDM LOO and kNNDM algorithms), 2) repetitively fitting the model according to the CV configuration, and 3) the total run-time, i.e. the sum of 1 and 2. We did that using the same simulation framework as in section 3.1 but with 50 different sample sizes, ranging from 100 to 4000 training points. We only used the strongly clustered and the random sampling designs for computational reasons. We used a maximum of 4000 training  
 195 points, since the computational time exceeded one week per run for NNDM LOO CV. The analysis was carried out using a high-performance computation cluster utilizing up to 1.5 GB of RAM for each run using the Intel® Xeon® Gold 6140 CPU.

The run-time analysis showed large speed gains of kNNDM CV compared to NNDM LOO CV under all tested sample designs (Figure 8). For the random sampling design, the kNNDM algorithm was especially fast due to the prior test for

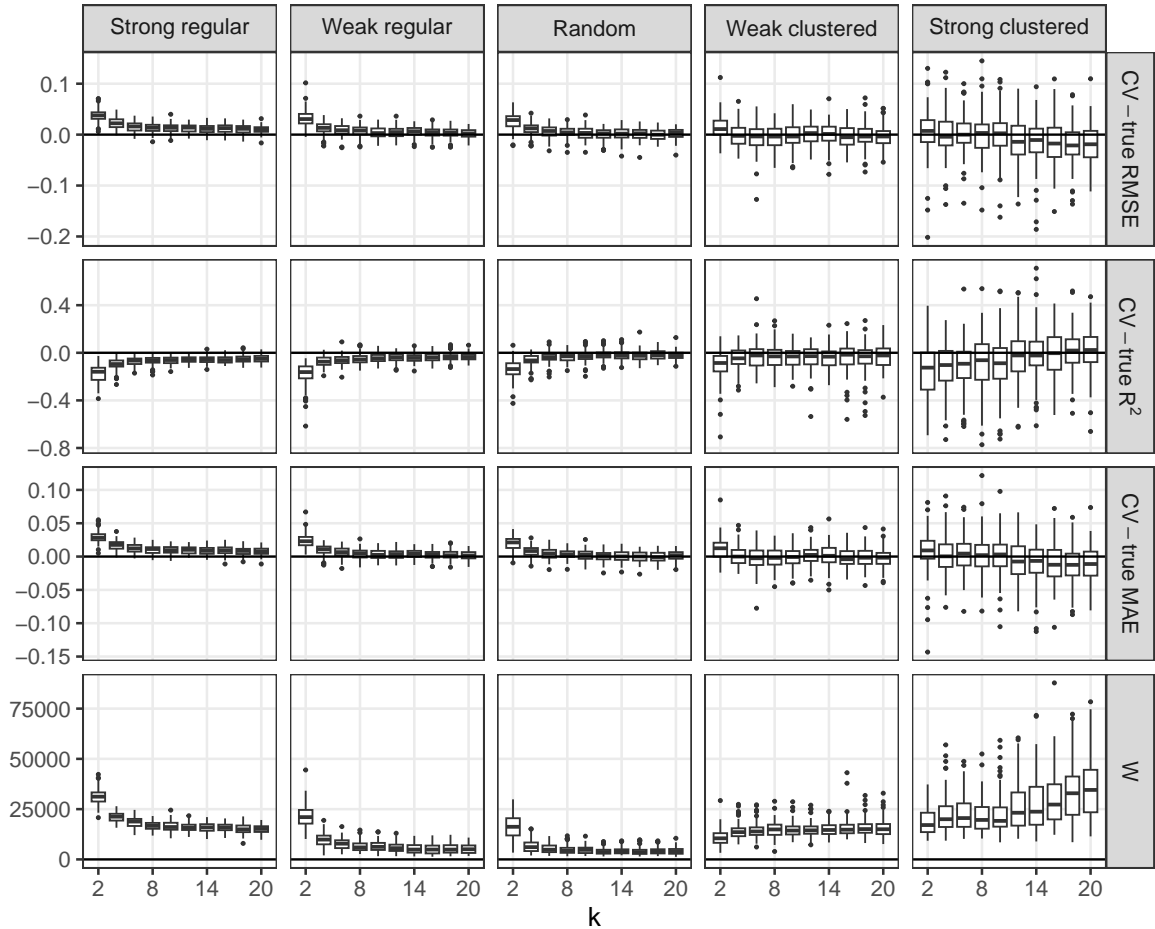


**Figure 7.** CV error estimates for kNNDM CV with different numbers of  $k$  (first three rows). The respective  $W$  statistic is shown in the fourth row.

clustering in the training data. This test returns a simple random  $k$ -fold CV when no clustering is detected, which is much  
 200 faster than running the entire kNNDM algorithm (see section 2). Only in four cases the test did not return a random CV, and in  
 those four cases the computational times were longer (red outliers in Figure 8).

NNDM LOO was slower compared to kNNDM when the training data were randomly distributed, and much slower when  
 they were clustered (Figure 8). Furthermore, the computational time of NNDM LOO CV increased exponentially with increas-  
 ing sample size. This pattern arises from both the architecture of the NNDM LOO CV algorithm (Figure 8 left column), and  
 205 from the difference between of LOO CV and  $k$ -fold CV in terms of model fitting, since NNDM LOO CV requires training  
 $k = N$  models while the number of models trained during  $k$ -fold CV is usually much smaller, in this case  $k = 10$  (Figure 8  
 middle column).

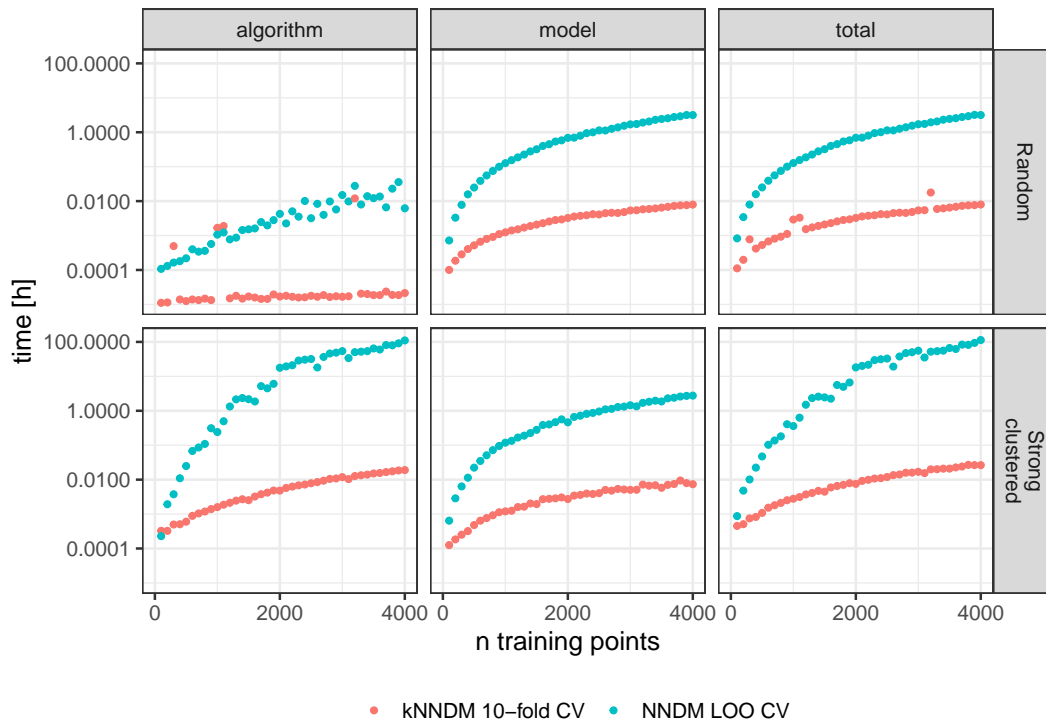


**Figure 8.** Differences in computational time (log-scaled) between 10-fold kNNDM CV (red) and NNDM LOO CV (blue) for two different sample designs (rows).

### 3.5 Additional simulation

To test the robustness of our results, we tested the performance of kNNDM CV in a second simulation using a real-world dataset described in detail the supporting methods and used in the study by de Bruin et al. (2022). Briefly, we modelled above-ground biomass in Europe using different sampling distributions ranging from regular to strongly clustered (Figure S1).

Results for the second simulation broadly agreed with the first simulation, although we observed some differences worth pointing out. 10-fold kNNDM reliably estimated the true RMSE in all designs except in the strongly clustered, where similar to spatial CV it resulted in overly optimistic estimates (Figure S2). The relationship between the absolute value difference between CV and true RMSE was positive but only explained a 28% explained of the total variance (Figure S3). While large numbers of folds resulted in a better match as expressed by  $W$  and more accurate RMSE for regular and random designs (Figure S4), in strongly clustered designs the opposite was observed. For weak clustered results,  $k = 4$  had the lowest  $W$  statistic although RMSE were also well estimated for larger values of  $k$ .

## 4 Discussion

220 In this work, we propose a new prediction-oriented CV strategy for map accuracy estimation named kNNDM that takes into account the geographical prediction space of the model. kNNDM extends the ideas of NNDM LOO CV (Milà et al., 2022) to a  $k$ -fold CV strategy that can be used for medium and even large reference datasets to estimate map accuracy in absence of probability sampling test data. In the simulation study, kNNDM performed similarly to NNDM LOO CV and produced reasonably reliable map accuracy estimates for most sampling patterns. Thus, kNNDM provided the advantages of our original  
225 NNDM LOO strategy while bypassing its sample size limitations. Small differences between NNDM LOO and kNNDM CV can be attributed to the different ways to match the distributions as well as the different hold-out sample size.

Similar to other studies (e.g. Wadoux et al., 2021; de Bruin et al., 2022), we observed that random  $k$ -fold CV returned reliable estimates of map accuracy with randomly distributed samples within the prediction area, while being overly optimistic when samples were clustered. Also in agreement with other studies, we found that spatial CV methods that do not take into  
230 account the geographical prediction space tended to be overly pessimistic even with clustered samples within the prediction area (Wadoux et al., 2021; de Bruin et al., 2022; Milà et al., 2022), for example as a result of block sizes that do not match the prediction task. A unique finding of our study that deserves special attention is the positive association we found between the  $W$  statistic measuring the quality of the match of the NND ECDFs during CV and prediction, and the quality of the estimation of the map accuracy statistics. This association was strong in our first simulation with a national scale, supporting our suggestion  
235 to design CV strategies that try to match the predictive conditions of the models in terms of geographical NND. That said, this relationship was weaker in the second simulation, where the study area had a continental scale. This suggests that other factors such as distances in the feature space may also play a role in the performance of CV map accuracy estimates.

Our experiments showed that the number of folds can have an impact on the performance of kNNDM. For randomly and regularly-distributed samples,  $k$  needs to be sufficiently large ( $k \geq 10$ ) to provide accurate estimates of map accuracy. The  
240 same finding applies to random  $k$ -fold CV, to which kNNDM generalises for random and regular samples. We attribute this to the fact that, when the number of clusters is small, neighbouring samples can be put in the same fold with a probability that increases with smaller  $k$ . On the other hand, for severely clustered samples, a smaller number of folds may be beneficial as  $k$  determines the maximum clustering that can be achieved when the geographical space is partitioned in  $k$  contiguous blocks. The suitability of a smaller number of folds was indicated by a higher quality of the match shown by the Wasserstein statistic.  
245 Comparing the suitability of different fold configurations via the Wasserstein statistic can be used for guidance when choosing the number of folds. Nonetheless, in clustered settings where  $W$  indicates that the best match is achieved by setting a very low  $k$  such as  $k=2$  (see Figure 7), we recommend taking a larger fold size such as 4 or 5 since the amount of bias expected with two folds due to large parts of the training data left out is expected to be large (Kohavi et al., 1995) and is likely the reason we observe better results for  $k=4$  or 6 in our experiments.

250 Even though kNNDM overcomes the sample size limitations of NNDM LOO CV, there are still limitations of the approach. First, the flexibility of the matching in kNNDM is lower than in NNDM LOO CV, since every observation must be assigned to a fold. Moreover, it is also possible that the range of NND observed during prediction is different than the range of NND

between training points, which might make the match impossible for some distances. This is especially the case when the prediction area is different from the training area (i.e. complete model transfer). Because of these reasons, the match between CV and prediction NND ECDF in kNNDM may not always be possible and an inspection of the NND ECDF like in Figure 1 should always be conducted. Similarly, if training data are very clustered within the prediction area as in the strongly clustered design of the second simulation, kNNDM may still fail to offer a CV configuration that matches the predictive conditions. In that case, we recommend users to allow for a greater maximum fold size, or ask for a lower fold number  $k$ , to account for potentially larger clusters. Furthermore, in cases where this is still not sufficient, we recommend restricting the prediction area to the area of applicability of the model (AOA, Meyer and Pebesma (2021)) to limit the effects of feature extrapolation. Secondly, both kNNDM and NNDM LOO CV algorithms are currently solely based on the geographical space; therefore, if the feature distribution between the training and prediction locations is very different, a feature-based CV strategy might be more appropriate (Roberts et al., 2017). For example, Wang et al. (2023) recently developed a CV method that considers both the geographic and feature space, although it does not consider the prediction domain and predictive conditions of the model. Thirdly, NNDM-based CV methods do not address the small error overestimation for regular samples we found in our simulations here or in Milà et al. (2022), so map accuracy estimates will tend to be slightly conservative in such cases. Fourthly, NNDM-based methods are purely based on geographical distances and ignore the location of the training points or the direction of the distances, which can be problematic if non-stationarity or anisotropy of the errors are present (Brenning, 2022). Fifthly, the CV error estimate obtained by kNNDM is only reasonable if the prediction area doesn't change when the model is deployed. If the prediction area changes significantly, re-evaluation might be required. Also, when the prediction area is unknown prior to model training, kNNDM cannot be used.

Possible future points for investigation regarding kNNDM include a simulation study comparing newly proposed CV-based map accuracy estimation methods (de Bruin et al., 2022) as well as feature-based CV methods (Roberts et al., 2017) in a larger variety of scenarios, also including classification problems, 2) implementing a genetic algorithm that minimizes the W statistic directly as a function of CV folds, 3) exploring the extension of kNNDM to feature space, and 4) investigating how kNNDM CV can affect feature selection (Meyer et al., 2019), hyperparameter tuning (Schratz et al., 2019), and model applicability (Meyer and Pebesma, 2021). A further possible extension to the kNNDM algorithm is the exclusion of training points during CV, which might help to achieve a better match in strongly clustered designs without the need to increase fold sizes. Furthermore, it might be beneficial to develop and integrate a one-sided Wasserstein test instead of using the Kolmogorov-Smirnov two-sample test to test whether the training points are clustered as the first step of the algorithm, since the Wasserstein test has a greater power than Kolmogorov-Smirnov's (Dowd, 2020) and would be also be more consistent with the rest of the algorithm, which also uses the Wasserstein statistic.

Finally, we would like to emphasize again that NNDM and kNNDM CV do not replace established strategies to estimate map accuracy via design based inference (as outlined in Wadoux et al., 2021), which should always be preferred. Nonetheless, prediction-oriented CV methods such as NNDM LOO or kNNDM CV that consider the prediction objectives of the model can be used to implement a measure of map accuracy during model development or, in absence of a probability sample, to estimate the map accuracy of a given model.

*Code availability.* All simulations were carried out in R v 4.2.1 (R Core Team, 2022). The most important packages used include `twosamples` (Dowd, 2022) for efficient calculation of the W statistic, `doParallel` (Corporation and Weston, 2022) for parallelization, `tidyverse` (Wickham et al., 2019) for data manipulation and `ggplot2` (Wickham, 2016) for data visualization. We used `sf` (Pebesma, 2018) for vector data operations, `terra` (Hijmans, 2023) for raster data operations and `caret` (Kuhn, 2022) for model fitting. NNDM LOO as well as the newly suggested kNNDM algorithms are implemented in the `CAST` package v 0.7.2 (Meyer et al., 2023). The code to perform the analysis and generate the figures included in the article is available at <https://doi.org/10.6084/m9.figshare.23514135.v1>, where the packages and the versions used for the simulations are listed.

295 *Author contributions.* All authors conceived the ideas and designed the study. JL and CM developed the algorithm, carried out the analysis, and drafted the manuscript. ML and HM contributed to discussions and drafts. All authors gave final approval for publication.

*Competing interests.* The authors declare no conflict of interest.

*Acknowledgements.* The work was supported by the Federal Ministry of Economic Affairs and Climate action of Germany (project number 50EE2009). CM was supported by a PhD fellowship of the *Severo Ochoa Centre of Excellence* programme awarded to ISGlobal.

## 300 References

- Baddeley, A., Rubak, E., and Turner, R.: Spatial point patterns: methodology and applications with R, CRC press, 2015.
- Beygelzimer, A., Kakadet, S., Langford, J., Arya, S., Mount, D., and Li, S.: FNN: Fast Nearest Neighbor Search Algorithms and Applications, <https://CRAN.R-project.org/package=FNN>, r package version 1.1.3.1, 2022.
- 305 Brenning, A.: Spatial cross-validation and bootstrap for the assessment of prediction rules in remote sensing: The R package sperrorest, in: 2012 IEEE International Geoscience and Remote Sensing Symposium, pp. 5372–5375, <https://doi.org/10.1109/IGARSS.2012.6352393>, 2012.
- Brenning, A.: Spatial machine-learning model diagnostics: a model-agnostic distance-based approach., International Journal of Geographical Information Science, <https://doi.org/10.1080/13658816.2022.2131789>, 2022.
- Conover, W. J.: Practical nonparametric statistics, vol. 350, john wiley & sons, 1999.
- 310 Corporation, M. and Weston, S.: doParallel: Foreach Parallel Adaptor for the 'parallel' Package, <https://CRAN.R-project.org/package=doParallel>, r package version 1.0.17, 2022.
- de Bruin, S., Brus, D. J., Heuvelink, G. B., van Ebbenhorst Tengbergen, T., and Wadoux, A. M.-C.: Dealing with clustered samples for assessing map accuracy by cross-validation, Ecological Informatics, 69, 101 665, <https://doi.org/10.1016/j.ecoinf.2022.101665>, 2022.
- Dowd, C.: A New ECDF Two-Sample Test Statistic, <https://doi.org/10.48550/ARXIV.2007.01360>, 2020.
- 315 Dowd, C.: twosamples: Fast Permutation Based Two Sample Tests, <https://CRAN.R-project.org/package=twosamples>, r package version 2.0.0, 2022.
- Hastie, T., Tibshirani, S., and Friedman, H.: The Elements of Statistical Learning. Data Mining, Inference, and Prediction., Springer Science & Business Media, 2009.
- Hengl, T., Mendes de Jesus, J., Heuvelink, G. B. M., Ruiperez Gonzalez, M., Kilibarda, M., Blagotic, A., Shangguan, W., Wright, M. N., 320 Geng, X., Bauer-Marschallinger, B., Guevara, M. A., Vargas, R., MacMillan, R. A., Batjes, N. H., Leenaars, J. G. B., Ribeiro, E., Wheeler, I., Mantel, S., and Kempen, B.: SoilGrids250m: Global gridded soil information based on machine learning., PloS one, 12, e0169748, place: United States, 2017.
- Hijmans, R. J.: terra: Spatial Data Analysis, <https://CRAN.R-project.org/package=terra>, r package version 1.7-3, 2023.
- Kohavi, R. et al.: A study of cross-validation and bootstrap for accuracy estimation and model selection, in: Ijcai, vol. 14, pp. 1137–1145, 325 Montreal, Canada, 1995.
- Kuhn, M.: caret: Classification and Regression Training, <https://CRAN.R-project.org/package=caret>, r package version 6.0-93, 2022.
- Le Rest, K., Pinaud, D., Monestiez, P., Chadoeuf, J., and Bretagnolle, V.: Spatial leave-one-out cross-validation for variable selection in the presence of spatial autocorrelation, Global Ecology and Biogeography, 23, 811–820, <https://doi.org/10.1111/geb.12161>, 2014.
- 330 Leroy, B., Meynard, C. N., Bellard, C., and Courchamp, F.: virtualspecies, an R package to generate virtual species distributions, Ecography, <https://doi.org/10.1111/ecog.01388>, 2015.
- Ludwig, M., Moreno-Martinez, , Hölzel, N., Pebesma, E., and Meyer, H.: Assessing and improving the transferability of current global spatial prediction models, Global Ecology and Biogeography, n/a, <https://doi.org/10.1111/geb.13635>, 2023.
- Martin, L. J., Blossey, B., and Ellis, E.: Mapping where ecologists work: biases in the global distribution of terrestrial ecological observations, 335 Frontiers in Ecology and the Environment, 10, 195–201, <https://doi.org/10.1890/110154>, 2012.



- Meyer, H. and Pebesma, E.: Predicting into unknown space? Estimating the area of applicability of spatial prediction models, *Methods in Ecology and Evolution*, <https://doi.org/https://doi.org/10.1111/2041-210X.13650>, 2021.
- Meyer, H. and Pebesma, E.: Machine learning-based global maps of ecological variables and the challenge of assessing them, *Nature Communications*, 13, 2208, 2022.
- 340 Meyer, H., Reudenbach, C., Wöllauer, S., and Nauss, T.: Importance of spatial predictor variable selection in machine learning applications – Moving from data reproduction to spatial prediction, *Ecological Modelling*, 411, 108 815, <https://doi.org/https://doi.org/10.1016/j.ecolmodel.2019.108815>, 2019.
- Meyer, H., Milà, C., Ludwig, M., and Linnenbrink, J.: CAST: 'caret' Applications for Spatial-Temporal Models, <https://github.com/HannaMeyer/CAST>, <https://hannameyer.github.io/CAST/>, 2023.
- 345 Milà, C., Mateu, J., Pebesma, E., and Meyer, H.: Nearest neighbour distance matching Leave-One-Out Cross-Validation for map validation, *Methods in Ecology and Evolution*, 13, 1304–1316, <https://doi.org/https://doi.org/10.1111/2041-210X.13851>, 2022.
- Moreno-Martínez, , Camps-Valls, G., Kattge, J., Robinson, N., Reichstein, M., Bodegom, P. v., Kramer, K., Cornelissen, J. H. C., Reich, P., Bahn, M., Niinemets, , Peñuelas, J., Craine, J. M., Cerabolini, B. E. L., Minden, V., Laughlin, D. C., Sack, L., Allred, B., Baraloto, C., Byun, C., Soudzilovskaia, N. A., and Running, S. W.: A methodology to derive global maps of leaf traits using remote sensing and climate data, *Remote Sensing of Environment*, 218, 69–88, <https://doi.org/https://doi.org/10.1016/j.rse.2018.09.006>, 2018.
- 350 Pebesma, E.: Simple Features for R: Standardized Support for Spatial Vector Data, *The R Journal*, 10, 439–446, <https://doi.org/10.32614/RJ-2018-009>, 2018.
- Ploton, P., Mortier, F., Réjou-Méchain, M., Barbier, N., Picard, N., Rossi, V., Dormann, C., Cornu, G., Viennois, G., Bayol, N., Lyapustin, A., Gourlet-Fleury, S., and Pélissier, R.: Spatial validation reveals poor predictive performance of large-scale ecological mapping models, *Ecography*, 43, 11, 4540, <https://doi.org/10.1038/s41467-020-18321-y>, 2020.
- R Core Team: R: A Language and Environment for Statistical Computing, R Foundation for Statistical Computing, Vienna, Austria, <https://www.R-project.org/>, 2022.
- Roberts, D. R., Bahn, V., Ciuti, S., Boyce, M. S., Elith, J., Guillera-Arroita, G., Hauenstein, S., Lahoz-Monfort, J. J., Schröder, B., Thuiller, W., Warton, D. I., Wintle, B. A., Hartig, F., and Dormann, C. F.: Cross-validation strategies for data with temporal, spatial, hierarchical, or phylogenetic structure, *Ecography*, 40, 913–929, <https://doi.org/10.1111/ecog.02881>, 2017.
- 360 Sabatini, F. M., Jiménez-Alfaro, B., Jandt, U., Chytrý, M., Field, R., Kessler, M., Lenoir, J., Schrod, F., Wiser, S. K., Arfin Khan, M. A. S., Attorre, F., Cayuela, L., De Sanctis, M., Dengler, J., Haider, S., Hatim, M. Z., Indreica, A., Jansen, F., Pauchard, A., Peet, R. K., Petřík, P., Pillar, V. D., Sandel, B., Schmidt, M., Tang, Z., van Bodegom, P., Vassilev, K., Violle, C., Alvarez-Davila, E., Davidar, P., Dolezal, J., Hérault, B., Galán-de Mera, A., Jiménez, J., Kambach, S., Kepfer-Rojas, S., Kreft, H., Lezama, F., Linares-Palomino, R., Monteagudo Mendoza, A., N'Dja, J. K., Phillips, O. L., Rivas-Torres, G., Sklenář, P., Speziale, K., Strohbach, B. J., Vásquez Martínez, R., Wang, H.-F., Wesche, K., and Bruelheide, H.: Global patterns of vascular plant alpha diversity, *Nature Communications*, 13, 4683, <https://doi.org/10.1038/s41467-022-32063-z>, 2022.
- Schratz, P., Muenchow, J., Iturrutxa, E., Richter, J., and Brenning, A.: Hyperparameter tuning and performance assessment of statistical and machine-learning algorithms using spatial data, *Ecological Modelling*, 406, 109–120, <https://doi.org/https://doi.org/10.1016/j.ecolmodel.2019.06.002>, 2019.
- 370 Stehman, S. V., Pengra, B. W., Horton, J. A., and Wellington, D. F.: Validation of the U.S. Geological Survey's Land Change Monitoring, Assessment and Projection (LCMAP) Collection 1.0 annual land cover products 1985–2017, *Remote Sensing of Environment*, 265, 112 646, <https://doi.org/https://doi.org/10.1016/j.rse.2021.112646>, 2021.

- Telford, R. and Birks, H.: Evaluation of transfer functions in spatially structured environments, *Quaternary Science Reviews*, 28, 1309 – 375 1316, <https://doi.org/https://doi.org/10.1016/j.quascirev.2008.12.020>, 2009.
- Valavi, R., Elith, J., Lahoz-Monfort, J. J., and Guillera-Arroita, G.: blockCV: An r package for generating spatially or environmentally separated folds for k-fold cross-validation of species distribution models, *Methods in Ecology and Evolution*, 10, 225–232, <https://doi.org/10.1111/2041-210X.13107>, 2019.
- van den Hoogen, J., Geisen, S., Routh, D., Ferris, H., Traunspurger, W., Wardle, D. A., de Goede, R. G. M., Adams, B. J., Ahmad, W., 380 Andriuzzi, W. S., Bardgett, R. D., Bonkowski, M., Campos-Herrera, R., Cares, J. E., Caruso, T., de Brito Caixeta, L., Chen, X., Costa, S. R., Creamer, R., Mauro da Cunha Castro, J., Dam, M., Djigal, D., Escuer, M., Griffiths, B. S., Gutiérrez, C., Hohberg, K., Kalinkina, D., Kardol, P., Kergunteuil, A., Korthals, G., Krashevskaya, V., Kudrin, A. A., Li, Q., Liang, W., Magilton, M., Marais, M., Martín, J. A. R., Matveeva, E., Mayad, E. H., Mulder, C., Mullin, P., Neilson, R., Nguyen, T. A. D., Nielsen, U. N., Okada, H., Rius, J. E. P., Pan, K., Peneva, V., Pellissier, L., Carlos Pereira da Silva, J., Pitteloud, C., Powers, T. O., Powers, K., Quist, C. W., Rasmann, S., Moreno, S. S., 385 Scheu, S., Setälä, H., Sushchuk, A., Tiunov, A. V., Trap, J., van der Putten, W., Vestergård, M., Villenave, C., Waeyenberge, L., Wall, D. H., Wilschut, R., Wright, D. G., Yang, J.-i., and Crowther, T. W.: Soil nematode abundance and functional group composition at a global scale, 572, 194–198, <https://doi.org/10.1038/s41586-019-1418-6>, number: 7768 Publisher: Nature Publishing Group, 2019.
- Vaserstein, L. N.: Markov processes over denumerable products of spaces, describing large systems of automata, *Problemy Peredachi Informatsii*, 5, 64–72, 1969.
- 390 Wadoux, A. M.-C., Heuvelink, G. B., de Bruin, S., and Brus, D. J.: Spatial cross-validation is not the right way to evaluate map accuracy, *Ecological Modelling*, 457, 109 692, <https://doi.org/https://doi.org/10.1016/j.ecolmodel.2021.109692>, 2021.
- Wang, Y., Khodadadzadeh, M., and Zurita-Milla, R.: Spatial+: A new cross-validation method to evaluate geospatial machine learning models, *International Journal of Applied Earth Observation and Geoinformation*, 121, 103 364, <https://doi.org/https://doi.org/10.1016/j.jag.2023.103364>, 2023.
- 395 Webster, R. and Oliver, M. A.: *Geostatistics for environmental scientists*, John Wiley & Sons, 2007.
- Wenger, S. J. and Olden, J. D.: Assessing transferability of ecological models: an underappreciated aspect of statistical validation, *Methods in Ecology and Evolution*, 3, 260–267, <https://doi.org/10.1111/j.2041-210X.2011.00170.x>, 2012.
- Wickham, H.: *ggplot2: Elegant Graphics for Data Analysis*, Springer-Verlag New York, <https://ggplot2.tidyverse.org>, 2016.
- Wickham, H., Averick, M., Bryan, J., Chang, W., McGowan, L. D., François, R., Grolemund, G., Hayes, A., Henry, L., Hester, J., Kuhn, M., 400 Pedersen, T. L., Miller, E., Bache, S. M., Müller, K., Ooms, J., Robinson, D., Seidel, D. P., Spinu, V., Takahashi, K., Vaughan, D., Wilke, C., Woo, K., and Yutani, H.: Welcome to the tidyverse, *Journal of Open Source Software*, 4, 1686, <https://doi.org/10.21105/joss.01686>, 2019.